Branching fraction measurement of the decay $B^+ \to \psi(2S)\phi(1020)K^+$

R. Aaij *et al.*[*]
(LHCb Collaboration)

(Received 5 March 2025; accepted 17 April 2025; published 13 May 2025)

The branching fraction of the decay $B^+ \to \psi(2S)\phi(1020)K^+$, relative to the topologically similar decay $B^+ \to J/\psi\phi(1020)K^+$, is measured using proton-proton collision data collected by the LHCb experiment at center-of-mass energies of 7, 8, and 13 TeV, corresponding to an integrated luminosity of 9 fb^{-1}. The ratio is found to be $0.061 \pm 0.004 \pm 0.009$, where the first uncertainty is statistical and the second systematic. Using the world-average branching fraction for $B^+ \to J/\psi\phi(1020)K^+$, the branching fraction for the decay $B^+ \to \psi(2S)\phi(1020)K^+$ is found to be $(3.0 \pm 0.2 \pm 0.5 \pm 0.2) \times 10^{-6}$, where the first uncertainty is statistical, the second systematic, and the third is due to the branching fraction of the normalization channel.

DOI: 10.1103/PhysRevD.111.092008

I. INTRODUCTION

The $B^+ \to \psi(2S)\phi K^+$ decay proceeds through the same quark transition $b \to c\bar{c}s$ as the topologically similar $B^+ \to J/\psi\phi K^+$ decay.[1] In the latter, states compatible with exotic mesons have been observed, such as the $\chi_{c1}(4140)$ state [1–4] and the $T_{c\bar{c}\bar{1}(4000)}$ state [5].[2] The $B^+ \to \psi(2S)\phi K^+$ phase space is about 80 times smaller than that of the $B^+ \to J/\psi\phi K^+$ decay, while the branching fraction $\mathcal{B}(B^+ \to \psi(2S)\phi K^+)$ is about 15 times smaller than that of the $B^+ \to J/\psi\phi K^+$ decay [7]. The average amplitude of the former process is therefore greater than that of the latter process. Thus, the $B^+ \to \psi(2S)\phi K^+$ decay provides the potential to make observations of high-mass resonant contributions that are complementary to those observed in the decay $B^+ \to J/\psi\phi K^+$, such as the $\chi_c(4700)$ state [8,9].

This paper presents a measurement of the branching fraction of the decay $B^+ \to \psi(2S)\phi K^+$ relative to the normalization decay $B^+ \to J/\psi\phi K^+$. The intermediate resonances are reconstructed as $\psi(2S) \to \mu^+\mu^-$, $J/\psi \to \mu^+\mu^-$, and $\phi \to K^+K^-$. This analysis uses the full Run 1 (2011–2012) and Run 2 (2015–2016, 2017, and 2018) LHCb data samples of proton-proton (pp) collisions at center-of-mass energies of 7, 8, and 13 TeV, corresponding to an integrated luminosity of about 9 fb^{-1}. The branching fraction of $B^+ \to \psi(2S)\phi K^+$, calculated using the $\mathcal{B}(B^+ \to J/\psi\phi K^+)$ value provided by the PDG [6], is also reported. This LHCb result is compared with a measurement of the branching fraction of $B^+ \to \psi(2S)\phi K^+$ reported by the CMS Collaboration [7].

II. DETECTOR AND SIMULATION

The LHCb detector [10,11] is a single-arm forward spectrometer covering the pseudorapidity range $2 < \eta < 5$, designed for the study of particles containing b or c quarks. The detector includes a high-precision tracking system consisting of a silicon-strip vertex detector surrounding the pp interaction region [12], a large-area silicon-strip detector located upstream of a dipole magnet with a bending power of about 4 Tm, and three stations of silicon-strip detectors and straw drift tubes [13,14] placed downstream of the magnet. The tracking system provides a measurement of the momentum p of charged particles with a relative uncertainty that varies from 0.5% at low momentum to 1.0% at 200 GeV/c. The minimum distance of a track to a primary vertex (PV), the impact parameter (IP), is measured with a resolution of $(15 + 29/p_{\mathrm{T}})$ μm, where p_{T} is the component of the momentum transverse to the beam, in GeV/c. Different types of charged hadrons are distinguished using information from two ring-imaging Cherenkov detectors [15]. Photons, electrons, and hadrons are identified by a calorimeter system consisting of scintillating-pad and preshower detectors, an electromagnetic and a hadronic calorimeter. Muons are identified by a system composed of alternating layers of iron and multiwire proportional chambers [16]. The online event selection

[*]Full author list given at end of the article.

[1]Throughout this paper inclusion of the charge-conjugated decays is implied and the $\phi(1020)$ is referred to as ϕ.

[2]In this paper the new PDG naming conventions [6] for exotic hadrons are used. The states formerly known as the $X(4140)$, $Z_{cs}^+(4000)$, and $X(4700)$ are now referred to as the $\chi_{c1}(4140)$, $T_{c\bar{c}\bar{s}\,1}(4000)$, and $\chi_c(4700)$, respectively.

is performed by a trigger [17], which consists of a hardware stage, based on information from the calorimeter and muon systems, followed by a two-level software stage, which applies a full event reconstruction. Between the two software stages, an alignment and calibration of the detector is performed in near real time and their results are used in the trigger [18]. The same alignment and calibration information is propagated to the off-line reconstruction software to ensure consistency and avoid additional systematic uncertainties that would be required were they different.

Simulation is required to model the effects of the detector acceptance and the selection requirements. In the simulation, pp collisions are generated using Pythia [19] with a specific LHCb configuration [20]. Decays of unstable particles are described by EvtGen [21], in which final-state radiation is generated using Photos [22]. The interaction of the generated particles with the detector, and its response, are implemented using the Geant4 toolkit [23] as described in Ref. [24].

III. BRANCHING FRACTION MEASUREMENT

The ratio of branching fractions $\mathcal{R}_{\rm BF}$ is measured as

$$\mathcal{R}_{\rm BF} \equiv \frac{\mathcal{B}(B^+ \to \psi(2S)\phi K^+)}{\mathcal{B}(B^+ \to J/\psi\phi K^+)} = \frac{N_{\rm Signal}}{N_{\rm Norm}}\frac{F_{\rm Signal}}{F_{\rm Norm}}\frac{\epsilon_{\rm Norm}}{\epsilon_{\rm Signal}}\frac{\mathcal{B}(J/\psi \to \mu^+\mu^-)}{\mathcal{B}(\psi(2S) \to \mu^+\mu^-)}, \quad (1)$$

where $\mathcal{B}(J/\psi \to \mu^+\mu^-) = (5.961 \pm 0.033)\%$ and $\mathcal{B}(B^+ \to J/\psi\phi K^+) = (5.0 \pm 0.4) \times 10^{-5}$ are the world-average branching fractions [6]. Assuming lepton flavor universality of the electroweak interaction, the branching fraction of the $\psi(2S) \to \mu^+\mu^-$ decay can be replaced by that of the $\psi(2S) \to e^+e^-$ decay, equal to $(0.793 \pm 0.017)\%$ [6], which has an uncertainty approximately 3 times smaller. The number of B^+ decays for the signal (normalization) mode with a charmonium decay combined with three kaons, including sidebands for the ϕ candidates in the K^+K^- mass spectra, is denoted by $N_{\rm Signal(Norm)}$. This is measured by fitting the B^+ meson mass distribution. The fraction of candidates in the K^+K^- invariant-mass spectrum attributed to the ϕ decays is denoted by $F_{\rm Signal(Norm)}$ and is obtained by fitting the K^+K^- mass distribution. Finally, $\epsilon_{\rm Signal(Norm)}$ is the efficiency of the signal (normalization) channel and is obtained from simulation.

A. Selection

Candidate $B^+ \to \psi(2S)\phi K^+$ signal and $B^+ \to J/\psi\phi K^+$ normalization decays are selected using a hardware trigger, a two-stage software trigger, and off-line event reconstruction criteria followed by two boosted decision tree (BDT) [25,26] classifiers that suppress background significantly. Selection criteria are identical for both channels, with the exception of the dimuon mass windows for the ψ, where ψ denotes either the $\psi(2S)$ or the J/ψ meson.

The hardware trigger selects events with at least one high-$p_{\rm T}$ muon candidate later associated with the ψ in the B^+ decay or selects events independent of any track used in the decay. The first stage of the software trigger selects a pair of oppositely charged muons with high invariant mass or a muon with high $p_{\rm T}$ and high $\chi^2_{\rm IP}$ for each track (or composite particle). The variable $\chi^2_{\rm IP}$ is defined as the difference in the vertex-fit χ^2 of the primary-vertex fit reconstructed with and without the track under consideration. The second stage of the software trigger selects pairs of muons with invariant mass within 120 MeV/c^2 of the ψ mass that form vertices which are significantly detached from the closest primary vertex.

Off-line, B^+ meson candidates are formed from combinations of ψ candidates with three kaons where one of the K^+K^- pairs has an invariant mass between 1000 and 1040 MeV/c^2. The ψ windows are tightened to ± 100 MeV/c^2 around the nominal masses which induces negligible losses of efficiency. Kaon candidates are required to have $p_{\rm T}$ larger than 100 MeV/c, $\chi^2_{\rm IP} > 1$, and to have particle-identification signatures compatible with the kaon hypothesis. The ϕ candidates are formed from pairs of oppositely charged kaons that originate from a common vertex and have $p_{\rm T}$ greater than 200 MeV/c. The B^+ candidates are required to have good vertices, to have invariant masses within 60 MeV/c^2 of the nominal B^+ mass, and to have momentum vectors aligned with the B^+ line of flight. A vertex fit is performed constraining the ψ mass to its nominal value as given by the PDG [6] and requiring the B^+ momentum vector to point back to its primary vertex. Candidates satisfying these criteria are retained for further consideration.

Background is suppressed using two BDT classifiers [25,26] implemented in the TMVA toolkit [27]. The first classifier is trained using fully simulated $B^+ \to \psi(2S)\phi K^+$ samples as a proxy for the signal and events from the far-upper sideband [$5.8 < M(\psi(2S)\phi K^+) < 6.0$ GeV/c^2] as a proxy for the background. The variables with highest discrimination power are used as input to the classifier. There are 21 variables that include the $p_{\rm T}$ and $\chi^2_{\rm IP}$ of the kaons, muons, ψ, ϕ, and the B^+ candidates, the cosine of the angle between the B^+ momentum and the vector connecting the PV and the B^+ decay vertex, the sum of the $\chi^2_{\rm IP}$ of all final-state particles with respect to the PV, the vertex χ^2 of the B^+ candidate, and the B^+ decay time and its significance. The chosen BDT threshold corresponds to a signal efficiency close to 90% and a background rejection of about 99%.

After all previous steps, more than one $B^+ \to \psi(2S)\phi K^+$ candidate in a single event can satisfy the selection criteria. In almost all of these cases (around 30% and 3% of events in the signal and normalization channels, respectively), this

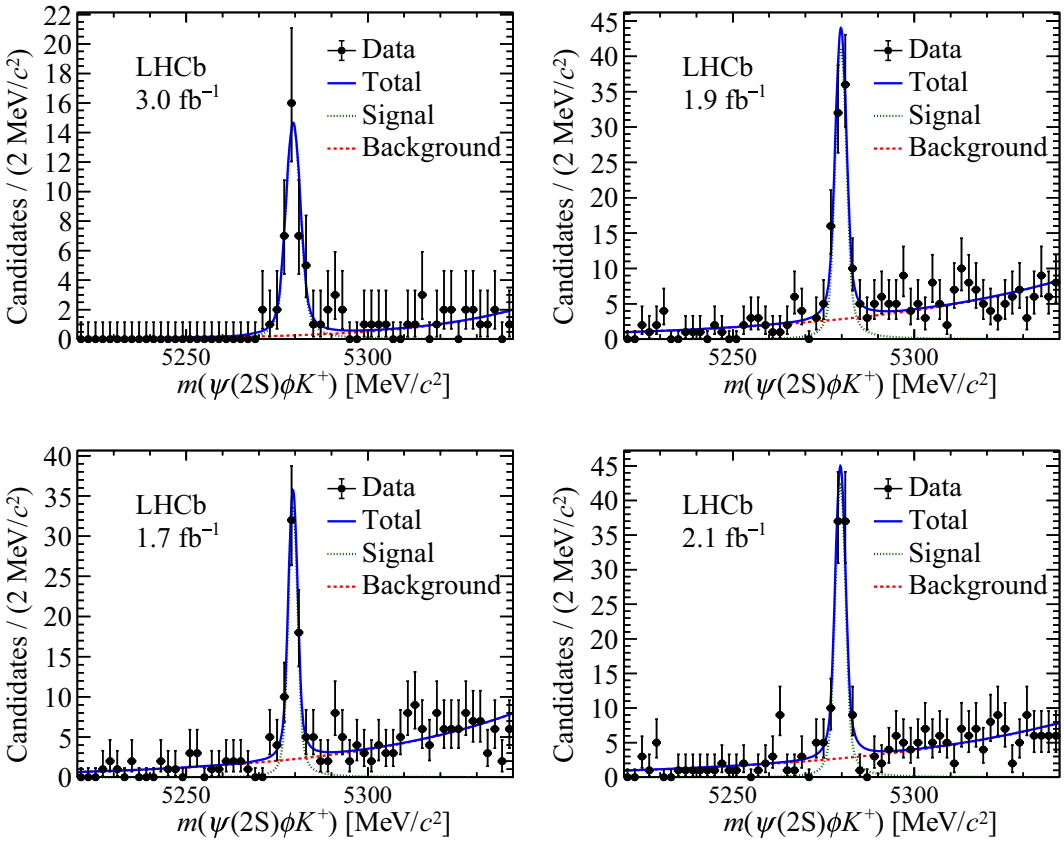

FIG. 1. Invariant-mass distributions of $B^+ \to \psi(2S)\phi K^+$ candidates with fit projections for (top left) Run 1, (top right) 2015–2016, (bottom left) 2017, and (bottom right) 2018 samples.

occurs when the masses of the two K^+K^- combinations in a single $B^+ \to \psi K^+K^-K^+$ candidate fall within the nominal ϕ window. Combinatorial background may also produce additional candidates in a single event, though on a smaller scale. To retain one B^+ candidate per event, a second BDT is trained with five variables as input. The input variables include properties of the B^+ meson, such as the $\chi^2_{\rm IP}$, the decay-time significance, the decay-vertex quality, the cosine of the angle between its momentum vector and the trajectory. Additionally, the input variables include the significance of the maximum distance between the trajectories of final-state particles. The candidate with the highest BDT output in each event is selected and its mass is used in the B^+ mass fit described below. The correlation between the mass of the B^+ candidate and the BDT output is found to be negligible. When the masses of both K^+K^- pairs in a $B^+ \to \psi K^+K^-K^+$ candidate fall within the nominal ϕ window, both K^+K^- combinations are used in the fit to determine $F_{\rm Signal}(F_{\rm Norm})$.

B. Mass fits

Unbinned maximum-likelihood mass fits are performed separately for the $B^+ \to \psi(2S)\phi K^+$ and $B^+ \to J/\psi\phi K^+$ samples and for each data-taking period as the detector operating conditions varied for each interval. For both the signal and normalization channels, the B^+ peak is modeled by a double-sided Crystal Ball function (DSCB) [28], while the background is described by an exponential function. The DSCB tail parameters are obtained from simulation and are fixed in the fits to the data. The yields of signal and background, the signal peak position M_{B^+} and width σ_{B^+}, and the parameters describing the exponential backgrounds are floated in the fits. Mass distributions of $B^+ \to \psi(2S)\phi K^+$ and $B^+ \to J/\psi\phi K^+$ candidates are shown in Figs. 1 and 2, respectively, along with the results of the fits. The fit parameters of each data-taking period are reported in Table I. The yields of the signal and normalization models determined from the fits over the combined samples are 289 ± 19 and 35315 ± 237 events, respectively, which are minimally compatible with the sum of the yields obtained independently, providing additional confidence in the consistency of these values.

Although the samples are selected with K^+K^- invariant masses in the 1000–1040 MeV/c^2 mass window, significant non-ϕ contributions are present. The fraction of ϕ candidates is obtained from a binned χ^2 fit to the extended K^+K^- mass distribution of 1000–1060 MeV/c^2. The selection criteria are the same as for the B^+ samples except for this relaxed K^+K^- mass range. In these fits, background is statistically

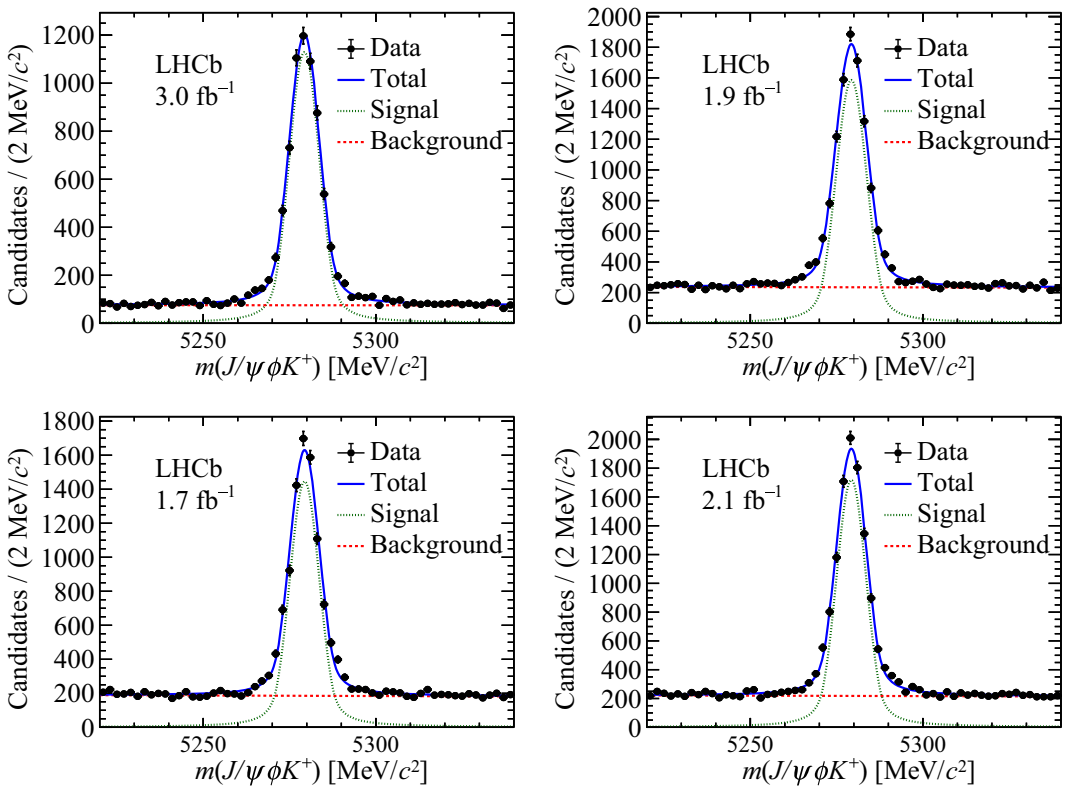

FIG. 2. Invariant-mass distribution of $B^+ \to J/\psi\phi K^+$ candidates with fit projections for (top left) Run 1, (top right) 2015–2016, (bottom left) 2017, and (bottom right) 2018 samples.

subtracted by means of the *sPlot* technique [29], using the results of the fit to the B^+ mass distributions. The mass distribution of the ϕ component is described by a P-wave Breit-Wigner function, convolved with a Gaussian function with resolution fixed to 1 MeV/c^2 (taken from simulation), while that of the non-ϕ component is described by an Argus function [30] whose parameters are floated. As the yields of signal in the disjoint data samples are small while the event-selection efficiency does not vary much in the K^+K^- mass window, both B^+ and K^+K^- mass fits are performed over the integrated Run 1 + Run 2 data samples. Therefore, only one $F_{\text{Signal(Norm)}}$ is calculated for each of the signal and normalization channels and used for all disjoint data samples. The K^+K^- mass fit results are shown in Fig. 3, in which the different line shapes of the non-ϕ component are mainly due to the different phase space of the signal and normalization modes. The fractions of ϕ contribution within the nominal K^+K^- mass window are determined to be

TABLE I. Results of the fit to the invariant mass of signal and normalization decays.

Period	Parameter	$B^+ \to \psi(2S)\phi K^+$	$B^+ \to J/\psi\phi K^+$
Run 1	M_{B^+} (MeV/c^2)	5279.45 ± 0.40	5279.30 ± 0.07
	σ_{B^+} (MeV/c^2)	2.04 ± 0.41	4.38 ± 0.07
	$N_{\text{Signal(Norm)}}$	43 ± 7	6835 ± 97
2015–2016	M_{B^+} (MeV/c^2)	5279.79 ± 0.22	5279.28 ± 0.06
	σ_{B^+} (MeV/c^2)	1.60 ± 0.23	4.46 ± 0.07
	$N_{\text{Signal(Norm)}}$	95 ± 11	9772 ± 129
2017	M_{B^+} (MeV/c^2)	5279.40 ± 0.22	5279.36 ± 0.06
	σ_{B^+} (MeV/c^2)	1.33 ± 0.23	4.26 ± 0.07
	$N_{\text{Signal(Norm)}}$	64 ± 9	8515 ± 118
2018	M_{B^+} (MeV/c^2)	5279.65 ± 0.19	5279.27 ± 0.06
	σ_{B^+} (MeV/c^2)	1.48 ± 0.16	4.29 ± 0.06
	$N_{\text{Signal(Norm)}}$	90 ± 11	10196 ± 128

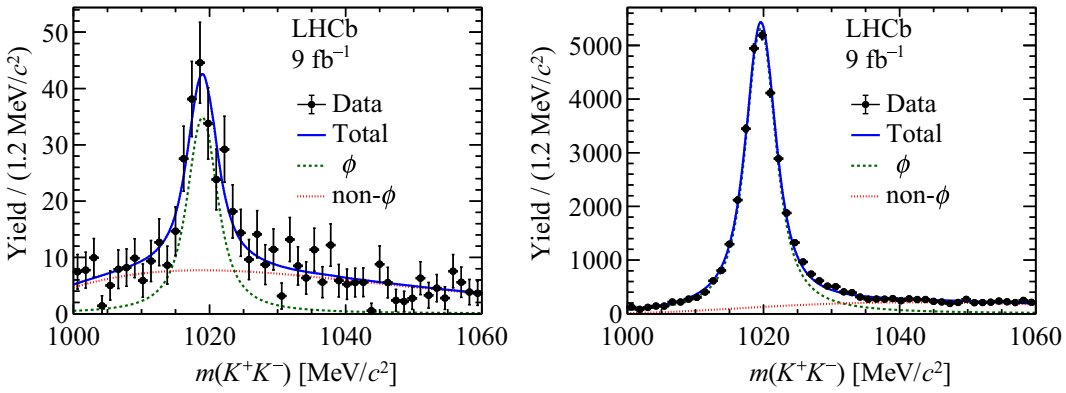

FIG. 3. Distributions of the background-subtracted K^+K^- mass spectra from the full (Run 1 + Run 2) data sample for (left) $B^+ \to \psi(2S)\phi K^+$ and (right) $B^+ \to J/\psi\phi K^+$ decays.

$F_{\text{Signal}} = 0.73 \pm 0.10$ and $F_{\text{Norm}} = 0.91 \pm 0.01$, where the uncertainties are statistical only. The values of χ^2 per degree of freedom for the signal and normalization fits are $\chi^2/\text{NDF} = 1.2$ and $\chi^2/\text{NDF} = 2.3$, respectively, both with the number of degrees of freedom NDF = 95.

C. Efficiencies

Particle-identification and tracking efficiencies are obtained from calibration data samples [31]. The remaining efficiencies, for both the signal and normalization decay modes, are obtained from simulated samples and calculated separately for each data-taking period. The normalization simulation sample, generated as pure phase space, is weighted to account for the structures in the $\psi\phi$ and ψK^+ masses observed in data. No similar correction has been applied to the signal simulation sample as no structure is visible in the Dalitz plot of the signal data sample. A systematic uncertainty is estimated to address possible residual effects. In the normalization sample, per-candidate weights are calculated by training a gradient-boosted decision-tree reweighter, GBReweighter, implemented in `hep_ml` [32]. The data distributions used here have the background subtracted statistically by means of the *sPlot* technique [29], using the results of the fit to the $B^+ \to J/\psi\phi K^+$ invariant-mass distribution.

Two factors distort the distribution of events in phase space (the ψ, ϕ, K^+ Dalitz plot), especially at the edges. First, the resolution of the reconstructed B^+ invariant mass cannot be neglected. To mitigate this problem, the masses of the B^+ and ψ candidates are constrained to their nominal values. Second, the natural line width of the ϕ meson cannot be neglected. Therefore, the simulated samples are reweighted in the $(s_{\psi K}, \cos(\theta))$ space, where s_{XY} denotes the invariant-mass squared of the XY system and θ is the angle between the ψ and ϕ, in the ϕK^+ rest frame, calculated as

$$\cos(\theta) = \frac{(m^2_{B^+} - s_{\phi K} - m^2_{\psi})(s_{\phi K} + m^2_{\phi} - m^2_{K}) + 2s_{\phi K}(m^2_{\psi} + m^2_{\phi} - s_{\psi\phi})}{\lambda^{\frac{1}{2}}(m^2_{B^+}, s_{\phi K}, m_{\psi})\lambda^{\frac{1}{2}}(s_{\phi K}, m^2_{\phi}, m^2_{K})}, \tag{2}$$

where m_{B^+}, m_{ψ}, and m_{ϕ} are the reconstructed mass of the B^+, ψ, and ϕ mesons, respectively, m_K is the known K^+ mass [6], and $\lambda^{\frac{1}{2}}(x, y, z)$ is defined as

$$\lambda^{\frac{1}{2}}(x, y, z) \equiv \sqrt{(x - y - z)(x - y - z) - 4yz}. \tag{3}$$

As this parametrization is not directly correlated with the ϕ mass, and $-1 < \cos(\theta) < 1$ by definition, the weighting at the limits of phase space is better behaved than if the usual Dalitz plot variables are used.

Ratios of efficiencies for the signal and normalization channels are derived from weighted, simulated data for each running period and are reported in Table II. Although the hardware and first-stage software triggers are more efficient for signal channel decays, the second-stage software trigger and off-line selection criteria are more efficient for the normalization channel decays. This results from the

TABLE II. Ratios of efficiencies for the signal and normalization channels for each data-taking period, as described in the text, where the uncertainties are statistical only.

Period	$\epsilon_{\text{Signal}}/\epsilon_{\text{Norm}}$
Run 1	0.823 ± 0.004
2015–2016	0.801 ± 0.007
2017	0.790 ± 0.004
2018	0.834 ± 0.003

TABLE III. Systematic uncertainties on the ratio of branching fractions of the decays $B^+ \to \psi(2S)\phi K^+$ and $B^+ \to J/\psi\phi K^+$, by origin and data-taking period.

Period	Mass model (%)	ϕ fraction (%)	Phase-space correction (%)	Simulation statistics (%)	Signal efficiency correction (%)	External inputs [6] (%)	Total (%)
Run 1	3	14	3	4	2	2	15
2015–2016	3	14	3	3	1	2	15
2017	3	14	3	3	3	2	15
2018	3	14	3	3	4	2	15
Combined	3	14	3	1	1	2	15

much smaller phase space for the kaons in the signal channel and the use of the track $\chi^2_{\rm IP}$ to exclude candidates with kaon momentum and B^+ flight directions consistent with each other.

D. Systematic uncertainties

Six sources of systematic uncertainty are discussed. Others were considered, but judged to be negligible compared to the statistical and overall systematic uncertainties reported.

The model used to describe the signal and background shapes may affect the results. Where the baseline fit uses a DSCB function to model the signal, a Johnson S_U function [33] is used as an alternative model to fit the data. Similarly, the baseline exponential background shape is replaced with a second order Chebyshev polynomial. Using the full dataset, results obtained with Johnson S_U show a difference of ∼2% in both signal and normalization samples. Added in quadrature, the total systematic uncertainty associated with the signal and background shapes is ∼3%.

The fractions of ϕ contributions in the nominal $m(K^+K^-)$ signal windows, $F_{\rm Signal}$ and $F_{\rm Norm}$, are also subject to fluctuation. Their statistical uncertainties are propagated to the branching fraction ratio measurements. These lead to a systematic effect of around 14%, almost entirely associated with the signal channel. This is the dominant systematic uncertainty. Increasing the uncertainty associated with $F_{\rm Norm}$ to account for the large χ^2/NDF value associated with its fit projection does not change the uncertainty in the ϕ fraction ratio at the level of precision reported.

The Breit-Wigner function used to model the ϕ mass distribution is not corrected for the $B^+ \to \psi K^- K^+ K^+$ four-body phase-space shape. Fitting the reweighted simulation samples with the same procedure yields a 3% deviation in the ratio of the fraction of ϕ events between signal and normalization samples.

The limited sizes of simulation samples lead to statistical uncertainties in the efficiencies. These are propagated to the final results as systematic uncertainties, explicitly accounting for the weighting procedure discussed below. The relative uncertainty from this source varies between 3% and 4%.

The weighting procedure accounting for resonant structure in phase space requires a set of four parameters as input to train the gradient-boosted decision-tree reweighter [32]. On trialing a large number of alternative parameter sets, the distribution of results shows a negligible spread. Therefore, no systematic uncertainty is associated with weighting the normalization channel. As the weighting procedure is not applied to the signal model in the baseline fit, the associated systematic uncertainty is estimated by taking the difference between the efficiency with and without this weighting. Uncertainties of 2%, 1%, 3%, and 4% are found for the Run 1, 2015–2016, 2017, and 2018 samples, respectively.

The branching fractions $\mathcal{B}(J/\psi \to \mu^+\mu^-)$ and $\mathcal{B}(\psi(2S) \to \mu^+\mu^-)$ are required to calculate the relative branching fraction $\mathcal{B}(B^+ \to \psi(2S)\phi K^+)/\mathcal{B}(B^+ \to J/\psi\phi K^+)$, and the branching fraction of the $B^+ \to J/\psi\phi K^+$ is additionally required for the $\mathcal{B}(B^+ \to \psi(2S)\phi K^+)$ calculation. These values are taken from the PDG [6] and their uncertainties are propagated to the final results. The contribution to the systematic uncertainty of the branching fraction ratio is ∼2% and the corresponding contribution to the $B^+ \to \psi(2S)\phi K^+$ branching fraction is ∼8%.

Table III summarizes the systematic uncertainties. With the exception of the uncertainties due to simulation sample sizes and signal weighting, systematic uncertainties are assumed to be fully correlated throughout all data-taking periods.

IV. RESULTS AND SUMMARY

Using the yields, the ϕ fractions, and efficiency ratios reported in Tables I and II, respectively, the ratio of branching fractions between the $B^+ \to \psi(2S)\phi K^+$ and $B^+ \to J/\psi\phi K^+$ decays is calculated. The results are reported in Table IV and illustrated in Fig. 4. The derived $B^+ \to \psi(2S)\phi K^+$ branching fraction results are illustrated in Fig. 5. Results for each data-taking period are combined using the Best Linear Unbiased Estimator method [34], which accounts for correlations among systematic effects. The reported results are consistent throughout the data-taking periods.

The combined value obtained for the ratio of branching fractions is

TABLE IV. Ratio of branching fractions $\mathcal{R}_{\rm BF}$ for each data-taking period and for the combined sample, where the first uncertainty is statistical and the second is systematic.

Period	$\mathcal{R}_{\rm BF}$
Run 1	$0.046 \pm 0.008 \pm 0.007$
2015–2016	$0.072 \pm 0.009 \pm 0.011$
2017	$0.056 \pm 0.008 \pm 0.008$
2018	$0.064 \pm 0.008 \pm 0.010$
Combined	$0.061 \pm 0.004 \pm 0.009$

$$\mathcal{R}_{\rm BF} \equiv \frac{\mathcal{B}(B^+ \to \psi(2S)\phi K^+)}{\mathcal{B}(B^+ \to J/\psi\phi K^+)} = 0.061 \pm 0.004 \pm 0.009,$$

where the first uncertainty is statistical and the second is systematic. The corresponding value for the $B^+ \to \psi(2S)\phi K^+$ branching fraction is

$$\mathcal{B}(B^+ \to \psi(2S)\phi K^+) = (3.0 \pm 0.2 \pm 0.5 \pm 0.2) \times 10^{-6},$$

where the third uncertainty is associated with the uncertainty of the branching fraction of the normalization channel. The result is compatible with the CMS measurement $(4.0 \pm 0.4 \pm 0.6 \pm 0.2) \times 10^{-6}$ [7].

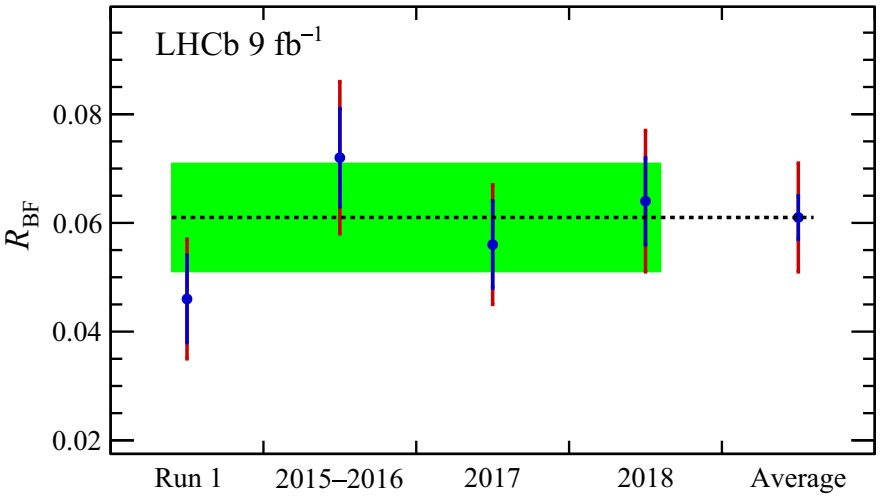

FIG. 4. Ratio $\mathcal{R}_{\rm BF}$ of branching fractions for the decays $B^+ \to \psi(2S)\phi K^+$ and $B^+ \to J/\psi\phi K^+$ for each data-taking period and the confidence level region at one standard deviation for the combined result in green. The inner error bars (in blue) and the outer error bars (in red) delimit the statistical and total (statistical plus systematic, added in quadrature) uncertainties, respectively.

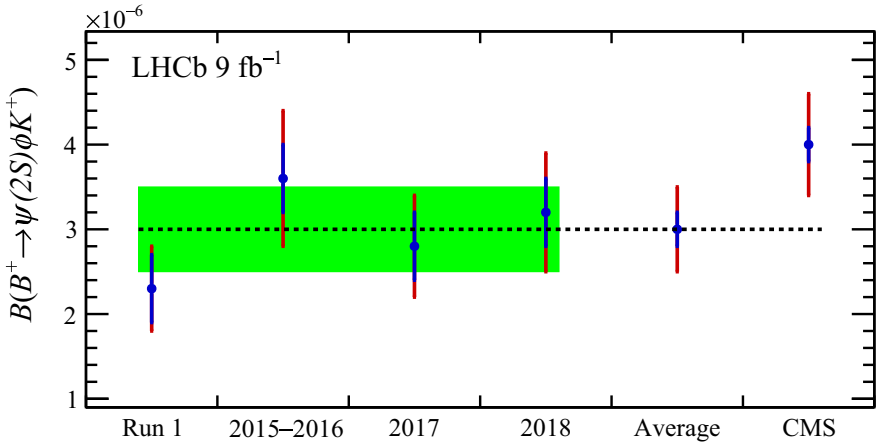

FIG. 5. Branching fraction of the decay $B^+ \to \psi(2S)\phi K^+$ for each data-taking period and the confidence level region at one standard deviation for the combined result in green. The inner error bars (in blue) and the outer error bars (in red) delimit the statistical and total (statistical plus systematic, added in quadrature) uncertainties, respectively. The CMS result [7] is included for comparison.

The phase space in $B^+ \to \psi(2S)\phi K^+$ decays is about 80 times smaller than that in $B^+ \to J/\psi\phi K^+$ decays. Considering Fermi's golden rule that the transition rate is proportional to the phase space times the magnitude of the amplitude squared, one may conclude that the average amplitude squared for the $B^+ \to \psi(2S)\phi K^+$ decay is approximately 5 times larger than that for the $B^+ \to J/\psi\phi K^+$ decay. This suggests the presence of resonant amplitudes in the $B^+ \to \psi(2S)\phi K^+$ decay that enhance its average decay rate. States such as the $\chi_c(4700)$ [8,9] have the right masses and quark content to play this role, so an amplitude analysis made possible with an increased data sample size represents a promising avenue for further investigation.

ACKNOWLEDGMENTS

We express our gratitude to our colleagues in the CERN accelerator departments for the excellent performance of the LHC. We thank the technical and administrative staff at the LHCb institutes. We acknowledge support from CERN and from the national agencies: ARC (Australia); CAPES, CNPq, FAPERJ, and FINEP (Brazil); MOST and NSFC (China); CNRS/IN2P3 (France); BMBF, DFG, and MPG (Germany); INFN (Italy); NWO (Netherlands); MNiSW and NCN (Poland); MCID/IFA (Romania); MICIU and AEI (Spain); SNSF and SER (Switzerland); NASU (Ukraine); STFC (United Kingdom); DOE NP and NSF (U.S.). We acknowledge the computing resources that are provided by ARDC (Australia), CBPF (Brazil), CERN, IHEP and LZU (China), IN2P3 (France), KIT and DESY (Germany), INFN (Italy), SURF (Netherlands), Polish WLCG (Poland), IFIN-HH (Romania), PIC (Spain), CSCS (Switzerland), and GridPP (United Kingdom). We are indebted to the communities behind the multiple open-source software packages on which we depend. Individual groups or members have received support from Key Research Program of Frontier Sciences of CAS, CAS PIFI, CAS CCEPP, Fundamental Research Funds for the Central Universities, and Science and Technology Program of Guangzhou (China); Minciencias (Colombia); EPLANET, Marie Skłodowska-Curie Actions, ERC and NextGenerationEU (European Union); A*MIDEX, ANR, IPhU, and Labex P2IO, and Région Auvergne-Rhône-Alpes (France); Alexander-von-Humboldt Foundation (Germany); ICSC (Italy); Severo Ochoa and María de Maeztu Units of Excellence, GVA, XuntaGal, GENCAT, InTalent-Inditex, and Prog. Atracción Talento CM (Spain); SRC (Sweden); the Leverhulme Trust, the Royal Society, and UKRI (United Kingdom).

DATA AVAILABILITY

The data supporting this study's findings are available within the article.

[1] T. Aaltonen *et al.* (CDF Collaboration), Evidence for a narrow near-threshold structure in the $J/\psi\phi$ mass spectrum in $B^+ \to J/\psi\phi K^+$ decays, Phys. Rev. Lett. **102**, 242002 (2009).
[2] S. Chatrchyan *et al.* (CMS Collaboration), Observation of a peaking structure in the $J/\psi\phi$ mass spectrum from $B^\pm \to J/\psi\phi K^\pm$ decays, Phys. Lett. B **734**, 261 (2014).
[3] V. M. Abazov *et al.* (D0 Collaboration), Search for the $X(4140)$ state in $B^+ \to J/\psi\phi K^+$ decays with the D0 detector, Phys. Rev. D **89**, 012004 (2014).
[4] R. Aaij *et al.* (LHCb Collaboration), Amplitude analysis of $B^+ \to J/\psi\phi K^+$ decays, Phys. Rev. D **95**, 012002 (2017).
[5] R. Aaij *et al.* (LHCb Collaboration), Observation of new resonances decaying to $J/\psi K^+$ and $J/\psi\phi$, Phys. Rev. Lett. **127**, 082001 (2021).
[6] S. Navas *et al.* (Particle Data Group), Review of particle physics, Phys. Rev. D **110**, 030001 (2024).
[7] V. Khachatryan *et al.* (CMS Collaboration), Observation of the decay $B^+ \to \psi(2S)\phi(1020)K^+$ in pp collisions at $\sqrt{s} = 8$ TeV, Phys. Lett. B **764**, 66 (2017).
[8] J. M. Dias, X. Liu, and M. Nielsen, Prediction for the decay width of a charged state near the $D_s\bar{D}^*/D_s^*\bar{D}$ threshold, Phys. Rev. D **88**, 096014 (2013).
[9] M. B. Voloshin, Strange hadrocharmonium, Phys. Lett. B **798**, 135022 (2019).
[10] A. A. Alves Jr. *et al.* (LHCb Collaboration), The LHCb detector at the LHC, J. Instrum. **3**, S08005 (2008).
[11] LHCb Collaboration, LHCb detector performance, Int. J. Mod. Phys. A **30**, 1530022 (2015).
[12] R. Aaij *et al.*, Performance of the LHCb vertex locator, J. Instrum. **9**, P09007 (2014).
[13] R. Arink *et al.*, Performance of the LHCb outer tracker, J. Instrum. **9**, P01002 (2014).
[14] P. d'Argent *et al.*, Improved performance of the LHCb outer tracker in LHC run 2, J. Instrum. **12**, P11016 (2017).
[15] M. Adinolfi *et al.*, Performance of the LHCb RICH detector at the LHC, Eur. Phys. J. C **73**, 2431 (2013).
[16] A. A. Alves Jr. *et al.*, Performance of the LHCb muon system, J. Instrum. **8**, P02022 (2013).
[17] R. Aaij *et al.*, The LHCb trigger and its performance in 2011, J. Instrum. **8**, P04022 (2013).
[18] G. Dujany and B. Storaci, Real-time alignment and calibration of the LHCb detector in run II, J. Phys. Conf. Ser. **664**, 082010 (2015).
[19] T. Sjöstrand, S. Mrenna, and P. Skands, A brief introduction to Pythia 8.1, Comput. Phys. Commun. **178**, 852 (2008);

T. Sjöstrand, S. Mrenna, and P. Skands, Pythia 6.4 physics and manual, J. High Energy Phys. 05 (2006) 026.
[20] I. Belyaev *et al.*, Handling of the generation of primary events in Gauss, the LHCb simulation framework, J. Phys. Conf. Ser. **331**, 032047 (2011).
[21] D. J. Lange, The EvtGen particle decay simulation package, Nucl. Instrum. Methods Phys. Res., Sect. A **462**, 152 (2001).
[22] N. Davidson, T. Przedzinski, and Z. Was, PHOTOS interface in C++: Technical and physics documentation, Comput. Phys. Commun. **199**, 86 (2016).
[23] J. Allison *et al.* (Geant4 Collaboration), Geant4 developments and applications, IEEE Trans. Nucl. Sci. **53**, 270 (2006); S. Agostinelli *et al.* (Geant4 Collaboration), Geant4: A simulation toolkit, Nucl. Instrum. Methods Phys. Res., Sect. A **506**, 250 (2003).
[24] M. Clemencic, G. Corti, S. Easo, C. R. Jones, S. Miglioranzi, M. Pappagallo, and P. Robbe, The LHCb simulation application, Gauss: Design, evolution and experience, J. Phys. Conf. Ser. **331**, 032023 (2011).
[25] L. Breiman, J. H. Friedman, R. A. Olshen, and C. J. Stone, *Classification and Regression Trees* (Wadsworth International Group, Belmont, California, USA, 1984).
[26] Y. Freund and R. E. Schapire, A decision-theoretic generalization of on-line learning and an application to boosting, J. Comput. Syst. Sci. **55**, 119 (1997).
[27] H. Voss, A. Hoecker, J. Stelzer, and F. Tegenfeldt, TMVA—toolkit for multivariate data analysis with ROOT, Proc. Sci. ACAT2007 (**2007**) 040; , TMVA 4—toolkit for multivariate data analysis with ROOT. Users guide, arXiv:physics/0703039.
[28] T. Skwarnicki, A study of the radiative cascade transitions between the Upsilon-prime and Upsilon resonances, Ph.D. thesis, Institute of Nuclear Physics, Krakow, 1986, DESY-F31-86-02.
[29] M. Pivk and F. R. Le Diberder, sPlot: A statistical tool to unfold data distributions, Nucl. Instrum. Methods Phys. Res., Sect. A **555**, 356 (2005).
[30] H. Albrecht *et al.* (ARGUS Collaboration), Search for hadronic $b \to u$ decays, Phys. Lett. B **241**, 278 (1990).
[31] R. Aaij *et al.*, Selection and processing of calibration samples to measure the particle identification performance of the LHCb experiment in Run 2, EPJ Tech. Instrum. **6**, 1 (2019).
[32] A. Rogozhnikov, Reweighting with boosted decision trees, J. Phys. Conf. Ser. **762**, 012036 (2016).
[33] N. L. Johnson, Systems of frequency curves generated by methods of translation, Biometrika **36**, 149 (1949).
[34] R. Nisius, BLUE: Combining correlated estimates of physics observables within ROOT using the best linear unbiased estimate method, SoftwareX **11**, 100468 (2020).

R. Aaij,[38] A. S. W. Abdelmotteleb,[57] C. Abellan Beteta,[51] F. Abudinén,[57] T. Ackernley,[61] A. A. Adefisoye,[69] B. Adeva,[47] M. Adinolfi,[55] P. Adlarson,[82] C. Agapopoulou,[14] C. A. Aidala,[83] Z. Ajaltouni,[11] S. Akar,[66] K. Akiba,[38] P. Albicocco,[28] J. Albrecht,[19,b] F. Alessio,[49] Z. Aliouche,[63] P. Alvarez Cartelle,[56] R. Amalric,[16] S. Amato,[3] J. L. Amey,[55] Y. Amhis,[14] L. An,[6] L. Anderlini,[27] M. Andersson,[51] A. Andreianov,[44] P. Andreola,[51] M. Andreotti,[26] D. Andreou,[69] A. Anelli,[31,c] D. Ao,[7] F. Archilli,[37,d] M. Argenton,[26] S. Arguedas Cuendis,[9,49] A. Artamonov,[44] M. Artuso,[69] E. Aslanides,[13] R. Ataíde Da Silva,[50] M. Atzeni,[65] B. Audurier,[12] D. Bacher,[64] I. Bachiller Perea,[10] S. Bachmann,[22] M. Bachmayer,[50] J. J. Back,[57] P. Baladron Rodriguez,[47] V. Balagura,[15] A. Balboni,[26] W. Baldini,[26] L. Balzani,[19] H. Bao,[7] J. Baptista de Souza Leite,[61] C. Barbero Pretel,[47,12] M. Barbetti,[27] I. R. Barbosa,[70] R. J. Barlow,[63] M. Barnyakov,[25] S. Barsuk,[14] W. Barter,[59] M. Bartolini,[56] J. Bartz,[69] J. M. Basels,[17] S. Bashir,[40] G. Bassi,[35,e] B. Batsukh,[5] P. B. Battista,[14] A. Bay,[50] A. Beck,[57] M. Becker,[19] F. Bedeschi,[35] I. B. Bediaga,[2] N. A. Behling,[19] S. Belin,[47] K. Belous,[44] I. Belov,[29] I. Belyaev,[36] G. Benane,[13] G. Bencivenni,[28] E. Ben-Haim,[16] A. Berezhnoy,[44] R. Bernet,[51] S. Bernet Andres,[46] A. Bertolin,[33] C. Betancourt,[51] F. Betti,[59] J. Bex,[56] Ia. Bezshyiko,[51] J. Bhom,[41] M. S. Bieker,[19] N. V. Biesuz,[26] P. Billoir,[16] A. Biolchini,[38] M. Birch,[62] F. C. R. Bishop,[10] A. Bitadze,[63] A. Bizzeti, T. Blake,[57] F. Blanc,[50] J. E. Blank,[19] S. Blusk,[69] V. Bocharnikov,[44] J. A. Boelhauve,[19] O. Boente Garcia,[15] T. Boettcher,[66] A. Bohare,[59] A. Boldyrev,[44] C. S. Bolognani,[79] R. Bolzonella,[26,f] R. B. Bonacci,[1] N. Bondar,[44] A. Bordelius,[49] F. Borgato,[33,g] S. Borghi,[63] M. Borsato,[31,c] J. T. Borsuk,[41] S. A. Bouchiba,[50] M. Bovill,[64] T. J. V. Bowcock,[61] A. Boyer,[49] C. Bozzi,[26] A. Brea Rodriguez,[50] N. Breer,[19] J. Brodzicka,[41] A. Brossa Gonzalo,[47,a] J. Brown,[61] D. Brundu,[32] E. Buchanan,[59] A. Buonaura,[51] L. Buonincontri,[33,g] A. T. Burke,[63] C. Burr,[49] J. S. Butter,[56] J. Buytaert,[49] W. Byczynski,[49] S. Cadeddu,[32] H. Cai,[74] A. Caillet,[16] R. Calabrese,[26,f] S. Calderon Ramirez,[9] L. Calefice,[45] S. Cali,[28] M. Calvi,[31,c] M. Calvo Gomez,[46] P. Camargo Magalhaes,[2,h] J. I. Cambon Bouzas,[47] P. Campana,[28] D. H. Campora Perez,[79] A. F. Campoverde Quezada,[7] S. Capelli,[31] L. Capriotti,[26] R. Caravaca-Mora,[9] A. Carbone,[25,i] L. Carcedo Salgado,[47] R. Cardinale,[29,j] A. Cardini,[32] P. Carniti,[31,c] L. Carus,[22] A. Casais Vidal,[65] R. Caspary,[22]

G. Casse,[61] M. Cattaneo,[49] G. Cavallero,[26,49] V. Cavallini,[26,f] S. Celani,[22] D. Cervenkov,[64] S. Cesare,[30,k] A. J. Chadwick,[61] I. Chahrour,[83] M. Charles,[16] Ph. Charpentier,[49] E. Chatzianagnostou,[38] M. Chefdeville,[10] C. Chen,[13] S. Chen,[5] Z. Chen,[7] A. Chernov,[41] S. Chernyshenko,[53] X. Chiotopoulos,[79] V. Chobanova,[81] S. Cholak,[50] M. Chrzaszcz,[41] A. Chubykin,[44] V. Chulikov,[28] P. Ciambrone,[28] X. Cid Vidal,[47] G. Ciezarek,[49] P. Cifra,[49] P. E. L. Clarke,[59] M. Clemencic,[49] H. V. Cliff,[56] J. Closier,[49] C. Cocha Toapaxi,[22] V. Coco,[49] J. Cogan,[13] E. Cogneras,[11] L. Cojocariu,[43] S. Collaviti,[50] P. Collins,[49] T. Colombo,[49] M. Colonna,[19] A. Comerma-Montells,[45] L. Congedo,[24] A. Contu,[32] N. Cooke,[60] I. Corredoira,[47] A. Correia,[16] G. Corti,[49] J. Cottee Meldrum,[55] B. Couturier,[49] D. C. Craik,[51] M. Cruz Torres,[2,l] E. Curras Rivera,[50] R. Currie,[59] C. L. Da Silva,[68] S. Dadabaev,[44] L. Dai,[71] X. Dai,[6] E. Dall'Occo,[49] J. Dalseno,[47] C. D'Ambrosio,[49] J. Daniel,[11] A. Danilina,[44] P. d'Argent,[24] G. Darze,[3] A. Davidson,[57] J. E. Davies,[63] A. Davis,[63] O. De Aguiar Francisco,[63] C. De Angelis,[32,m] F. De Benedetti,[49] J. de Boer,[38] K. De Bruyn,[78] S. De Capua,[63] M. De Cian,[22] U. De Freitas Carneiro Da Graca,[2,n] E. De Lucia,[28] J. M. De Miranda,[2] L. De Paula,[3] M. De Serio,[24,o] P. De Simone,[28] F. De Vellis,[19] J. A. de Vries,[79] F. Debernardis,[24] D. Decamp,[10] V. Dedu,[13] S. Dekkers,[1] L. Del Buono,[16] B. Delaney,[65] H.-P. Dembinski,[19] J. Deng,[8] V. Denysenko,[51] O. Deschamps,[11] F. Dettori,[32,m] B. Dey,[77] P. Di Nezza,[28] I. Diachkov,[44] S. Didenko,[44] S. Ding,[69] L. Dittmann,[22] V. Dobishuk,[53] A. D. Docheva,[60] C. Dong,[4,p] A. M. Donohoe,[23] F. Dordei,[32] A. C. dos Reis,[2] A. D. Dowling,[69] W. Duan,[72] P. Duda,[80] M. W. Dudek,[41] L. Dufour,[49] V. Duk,[34] P. Durante,[49] M. M. Duras,[80] J. M. Durham,[68] O. D. Durmus,[77] A. Dziurda,[41] A. Dzyuba,[44] S. Easo,[58] E. Eckstein,[18] U. Egede,[1] A. Egorychev,[44] V. Egorychev,[44] S. Eisenhardt,[59] E. Ejopu,[63] L. Eklund,[82] M. Elashri,[66] J. Ellbracht,[19] S. Ely,[62] A. Ene,[43] J. Eschle,[69] S. Esen,[22] T. Evans,[63] F. Fabiano,[32,m] L. N. Falcao,[2] Y. Fan,[7] B. Fang,[7] L. Fantini,[34,49,q] M. Faria,[50] K. Farmer,[59] D. Fazzini,[31,c] L. Felkowski,[80] M. Feng,[5,7] M. Feo,[19] A. Fernandez Casani,[48] M. Fernandez Gomez,[47] A. D. Fernez,[67] F. Ferrari,[25,i] F. Ferreira Rodrigues,[3] M. Ferrillo,[51] M. Ferro-Luzzi,[49] S. Filippov,[44] R. A. Fini,[24] M. Fiorini,[26,f] M. Firlej,[40] K. L. Fischer,[64] D. S. Fitzgerald,[83] C. Fitzpatrick,[63] T. Fiutowski,[40] F. Fleuret,[15] M. Fontana,[25] L. F. Foreman,[63] R. Forty,[49] D. Foulds-Holt,[56] V. Franco Lima,[3] M. Franco Sevilla,[67] M. Frank,[49] E. Franzoso,[26,f] G. Frau,[63] C. Frei,[49] D. A. Friday,[63] J. Fu,[7] Q. Führing,[19,56,b] Y. Fujii,[1] T. Fulghesu,[16] E. Gabriel,[38] G. Galati,[24] M. D. Galati,[38] A. Gallas Torreira,[47] D. Galli,[25,i] S. Gambetta,[59] M. Gandelman,[3] P. Gandini,[30] B. Ganie,[63] H. Gao,[7] R. Gao,[64] T. Q. Gao,[56] Y. Gao,[8] Y. Gao,[6] Y. Gao,[8] L. M. Garcia Martin,[50] P. Garcia Moreno,[45] J. García Pardiñas,[49] P. Gardner,[67] K. G. Garg,[8] L. Garrido,[45] C. Gaspar,[49] R. E. Geertsema,[38] L. L. Gerken,[19] E. Gersabeck,[63] M. Gersabeck,[20] T. Gershon,[57] S. Ghizzo,[29,j] Z. Ghorbanimoghaddam,[55] L. Giambastiani,[33,g] F. I. Giasemis,[16,r] V. Gibson,[56] H. K. Giemza,[42] A. L. Gilman,[64] M. Giovannetti,[28] A. Gioventù,[45] L. Girardey,[63,58] P. Gironella Gironell,[45] C. Giugliano,[26,f] M. A. Giza,[41] E. L. Gkougkousis,[62] F. C. Glaser,[14,22] V. V. Gligorov,[16,49] C. Göbel,[70] E. Golobardes,[46] D. Golubkov,[44] A. Golutvin,[62,49,44] S. Gomez Fernandez,[45] W. Gomulka,[40] F. Goncalves Abrantes,[64] M. Goncerz,[41] G. Gong,[4,p] J. A. Gooding,[19] I. V. Gorelov,[44] C. Gotti,[31] J. P. Grabowski,[18] L. A. Granado Cardoso,[49] E. Graugés,[45] E. Graverini,[50,s] L. Grazette,[57] G. Graziani, A. T. Grecu,[43] L. M. Greeven,[38] N. A. Grieser,[66] L. Grillo,[60] S. Gromov,[44] C. Gu,[15] M. Guarise,[26] L. Guerry,[11] M. Guittiere,[14] V. Guliaeva,[44] P. A. Günther,[22] A.-K. Guseinov,[50] E. Gushchin,[44] Y. Guz,[6,49,44] T. Gys,[49] K. Habermann,[18] T. Hadavizadeh,[1] C. Hadjivasiliou,[67] G. Haefeli,[50] C. Haen,[49] M. Hajheidari,[49] G. Hallett,[57] M. M. Halvorsen,[49] P. M. Hamilton,[67] J. Hammerich,[61] Q. Han,[8] X. Han,[22,49] S. Hansmann-Menzemer,[22] L. Hao,[7] N. Harnew,[64] T. H. Harris,[1] M. Hartmann,[14] S. Hashmi,[40] J. He,[7,t] F. Hemmer,[49] C. Henderson,[66] R. D. L. Henderson,[1,57] A. M. Hennequin,[49] K. Hennessy,[61] L. Henry,[50] J. Herd,[62] P. Herrero Gascon,[22] J. Heuel,[17] A. Hicheur,[3] G. Hijano Mendizabal,[51] J. Horswill,[63] R. Hou,[8] Y. Hou,[11] N. Howarth,[61] J. Hu,[72] W. Hu,[6] X. Hu,[4,p] W. Huang,[7] W. Hulsbergen,[38] R. J. Hunter,[57] M. Hushchyn,[44] D. Hutchcroft,[61] M. Idzik,[40] D. Ilin,[44] P. Ilten,[66] A. Inglessi,[44] A. Iniukhin,[44] A. Ishteev,[44] K. Ivshin,[44] R. Jacobsson,[49] H. Jage,[17] S. J. Jaimes Elles,[75,49,48] S. Jakobsen,[49] E. Jans,[38] B. K. Jashal,[48] A. Jawahery,[67,49] V. Jevtic,[19,b] E. Jiang,[67] X. Jiang,[5,7] Y. Jiang,[7] Y. J. Jiang,[6] M. John,[64] A. John Rubesh Rajan,[23] D. Johnson,[54] C. R. Jones,[56] T. P. Jones,[57] S. Joshi,[42] B. Jost,[49] J. Juan Castella,[56] N. Jurik,[49] I. Juszczak,[41] D. Kaminaris,[50] S. Kandybei,[52] M. Kane,[59] Y. Kang,[4,p] C. Kar,[11] M. Karacson,[49] D. Karpenkov,[44] A. Kauniskangas,[50] J. W. Kautz,[66] M. K. Kazanecki,[41] F. Keizer,[49] M. Kenzie,[56] T. Ketel,[38] B. Khanji,[69] A. Kharisova,[44] S. Kholodenko,[35,49]

G. Khreich,[14] T. Kirn,[17] V. S. Kirsebom,[31,c] O. Kitouni,[65] S. Klaver,[39] N. Kleijne,[35,e] K. Klimaszewski,[42] M. R. Kmiec,[42] S. Koliiev,[53] L. Kolk,[19] A. Konoplyannikov,[44] P. Kopciewicz,[40,49] P. Koppenburg,[38] M. Korolev,[44] I. Kostiuk,[38] O. Kot,[53] S. Kotriakhova, A. Kozachuk,[44] P. Kravchenko,[44] L. Kravchuk,[44] M. Kreps,[57] P. Krokovny,[44] W. Krupa,[69] W. Krzemien,[42] O. Kshyvanskyi,[53] S. Kubis,[80] M. Kucharczyk,[41] V. Kudryavtsev,[44] E. Kulikova,[44] A. Kupsc,[82] B. K. Kutsenko,[13] D. Lacarrere,[49] P. Laguarta Gonzalez,[45] A. Lai,[32] A. Lampis,[32] D. Lancierini,[56] C. Landesa Gomez,[47] J. J. Lane,[1] R. Lane,[55] G. Lanfranchi,[28] C. Langenbruch,[22] J. Langer,[19] O. Lantwin,[44] T. Latham,[57] F. Lazzari,[35,s] C. Lazzeroni,[54] R. Le Gac,[13] H. Lee,[61] R. Lefèvre,[11] A. Leflat,[44] S. Legotin,[44] M. Lehuraux,[57] E. Lemos Cid,[49] O. Leroy,[13] T. Lesiak,[41] E. D. Lesser,[49] B. Leverington,[22] A. Li,[4,p] C. Li,[13] H. Li,[72] K. Li,[8] L. Li,[63] M. Li,[8] P. Li,[7] P.-R. Li,[73] Q. Li,[5,7] S. Li,[8] T. Li,[5,u] T. Li,[72] Y. Li,[8] Y. Li,[5] Z. Lian,[4,p] X. Liang,[69] S. Libralon,[48] C. Lin,[7] T. Lin,[58] R. Lindner,[49] H. Linton,[62] V. Lisovskyi,[50] R. Litvinov,[32,49] F. L. Liu,[1] G. Liu,[72] K. Liu,[73] S. Liu,[5,7] W. Liu,[8] Y. Liu,[59] Y. Liu,[73] Y. L. Liu,[62] A. Lobo Salvia,[45] A. Loi,[32] T. Long,[56] J. H. Lopes,[3] A. Lopez Huertas,[45] S. López Soliño,[47] Q. Lu,[15] C. Lucarelli,[27] D. Lucchesi,[33,g] M. Lucio Martinez,[79] V. Lukashenko,[38,53] Y. Luo,[6] A. Lupato,[33,v] E. Luppi,[26,f] K. Lynch,[23] X.-R. Lyu,[7] G. M. Ma,[4,p] S. Maccolini,[19] F. Machefert,[14] F. Maciuc,[43] B. Mack,[69] I. Mackay,[64] L. M. Mackey,[69] L. R. Madhan Mohan,[56] M. J. Madurai,[54] A. Maevskiy,[44] D. Magdalinski,[38] D. Maisuzenko,[44] M. W. Majewski,[40] J. J. Malczewski,[41] S. Malde,[64] L. Malentacca,[49] A. Malinin,[44] T. Maltsev,[44] G. Manca,[32,m] G. Mancinelli,[13] C. Mancuso,[30,14,k] R. Manera Escalero,[45] F. M. Manganella,[37] D. Manuzzi,[25] D. Marangotto,[30,k] J. F. Marchand,[10] R. Marchevski,[50] U. Marconi,[25] E. Mariani,[16] S. Mariani,[49] C. Marin Benito,[45,49] J. Marks,[22] A. M. Marshall,[55] L. Martel,[64] G. Martelli,[34,q] G. Martellotti,[36] L. Martinazzoli,[49] M. Martinelli,[31,c] D. Martinez Gomez,[78] D. Martinez Santos,[81] F. Martinez Vidal,[48] A. Martorell i Granollers,[46] A. Massafferri,[2] R. Matev,[49] A. Mathad,[49] V. Matiunin,[44] C. Matteuzzi,[69] K. R. Mattioli,[15] A. Mauri,[62] E. Maurice,[15] J. Mauricio,[45] P. Mayencourt,[50] J. Mazorra de Cos,[48] M. Mazurek,[42] M. McCann,[62] L. Mcconnell,[23] T. H. McGrath,[63] N. T. McHugh,[60] A. McNab,[63] R. McNulty,[23] B. Meadows,[66] G. Meier,[19] D. Melnychuk,[42] F. M. Meng,[4,p] M. Merk,[38,79] A. Merli,[50] L. Meyer Garcia,[67] D. Miao,[5,7] H. Miao,[7] M. Mikhasenko,[76] D. A. Milanes,[75] A. Minotti,[31,c] E. Minucci,[28] T. Miralles,[11] B. Mitreska,[19] D. S. Mitzel,[19] A. Modak,[58] R. A. Mohammed,[64] R. D. Moise,[17] S. Mokhnenko,[44] E. F. Molina Cardenas,[83] T. Mombächer,[49] M. Monk,[57,1] S. Monteil,[11] A. Morcillo Gomez,[47] G. Morello,[28] M. J. Morello,[35,e] M. P. Morgenthaler,[22] J. Moron,[40] W. Morren,[38] A. B. Morris,[49] A. G. Morris,[13] R. Mountain,[69] H. Mu,[4,p] Z. M. Mu,[6] E. Muhammad,[57] F. Muheim,[59] M. Mulder,[78] K. Müller,[51] F. Muñoz-Rojas,[9] R. Murta,[62] P. Naik,[61] T. Nakada,[50] R. Nandakumar,[58] T. Nanut,[49] I. Nasteva,[3] M. Needham,[59] N. Neri,[30,k] S. Neubert,[18] N. Neufeld,[49] P. Neustroev,[44] J. Nicolini,[19,14] D. Nicotra,[79] E. M. Niel,[49] N. Nikitin,[44] Q. Niu,[73] P. Nogarolli,[3] P. Nogga,[18] C. Normand,[55] J. Novoa Fernandez,[47] G. Nowak,[66] C. Nunez,[83] H. N. Nur,[60] A. Oblakowska-Mucha,[40] V. Obraztsov,[44] T. Oeser,[17] S. Okamura,[26,f] A. Okhotnikov,[44] O. Okhrimenko,[53] R. Oldeman,[32,m] F. Oliva,[59] M. Olocco,[19] C. J. G. Onderwater,[79] R. H. O'Neil,[59] D. Osthues,[19] J. M. Otalora Goicochea,[3] P. Owen,[51] A. Oyanguren,[48] O. Ozcelik,[59] F. Paciolla,[35,w] A. Padee,[42] K. O. Padeken,[18] B. Pagare,[57] P. R. Pais,[22] T. Pajero,[49] A. Palano,[24] M. Palutan,[28] X. Pan,[4,p] G. Panshin,[44] L. Paolucci,[57] A. Papanestis,[58,49] M. Pappagallo,[24,o] L. L. Pappalardo,[26,f] C. Pappenheimer,[66] C. Parkes,[63] D. Parmar,[76] B. Passalacqua,[26,f] G. Passaleva,[27] D. Passaro,[35,e] A. Pastore,[24] M. Patel,[62] J. Patoc,[64] C. Patrignani,[25,i] A. Paul,[69] C. J. Pawley,[79] A. Pellegrino,[38] J. Peng,[5,7] M. Pepe Altarelli,[28] S. Perazzini,[25] D. Pereima,[44] H. Pereira Da Costa,[68] A. Pereiro Castro,[47] P. Perret,[11] A. Perrevoort,[78] A. Perro,[49,13] M. J. Peters,[66] K. Petridis,[55] A. Petrolini,[29,j] J. P. Pfaller,[66] H. Pham,[69] L. Pica,[35,e] M. Piccini,[34] L. Piccolo,[32] B. Pietrzyk,[10] G. Pietrzyk,[14] D. Pinci,[36] F. Pisani,[49] M. Pizzichemi,[31,49,c] V. Placinta,[43] M. Plo Casasus,[47] T. Poeschl,[49] F. Polci,[16,49] M. Poli Lener,[28] A. Poluektov,[13] N. Polukhina,[44] I. Polyakov,[44] E. Polycarpo,[3] S. Ponce,[49] D. Popov,[7] S. Poslavskii,[44] K. Prasanth,[59] C. Prouve,[81] D. Provenzano,[32,m] V. Pugatch,[53] G. Punzi,[35,s] S. Qasim,[51] Q. Q. Qian,[6] W. Qian,[7] N. Qin,[4,p] S. Qu,[4,p] R. Quagliani,[49] R. I. Rabadan Trejo,[57] J. H. Rademacker,[55] M. Rama,[35] M. Ramírez García,[83] V. Ramos De Oliveira,[70] M. Ramos Pernas,[57] M. S. Rangel,[3] F. Ratnikov,[44] G. Raven,[39] M. Rebollo De Miguel,[48] F. Redi,[30,v] J. Reich,[55] F. Reiss,[63] Z. Ren,[7] P. K. Resmi,[64] R. Ribatti,[50] G. Ricart,[15,12] D. Riccardi,[35,e] S. Ricciardi,[58] K. Richardson,[65] M. Richardson-Slipper,[59] K. Rinnert,[61] P. Robbe,[14,49] G. Robertson,[60]

E. Rodrigues,[61] A. Rodriguez Alvarez,[45] E. Rodriguez Fernandez,[47] J. A. Rodriguez Lopez,[75] E. Rodriguez Rodriguez,[47] J. Roensch,[19] A. Rogachev,[44] A. Rogovskiy,[58] D. L. Rolf,[49] P. Roloff,[49] V. Romanovskiy,[66] A. Romero Vidal,[47] G. Romolini,[26] F. Ronchetti,[50] T. Rong,[6] M. Rotondo,[28] S. R. Roy,[22] M. S. Rudolph,[69] M. Ruiz Diaz,[22] R. A. Ruiz Fernandez,[47] J. Ruiz Vidal,[82,x] A. Ryzhikov,[44] J. Ryzka,[40] J. J. Saavedra-Arias,[9] J. J. Saborido Silva,[47] R. Sadek,[15] N. Sagidova,[44] D. Sahoo,[77] N. Sahoo,[54] B. Saitta,[32,m] M. Salomoni,[31,49,c] I. Sanderswood,[48] R. Santacesaria,[36] C. Santamarina Rios,[47] M. Santimaria,[28,49] L. Santoro,[2] E. Santovetti,[37] A. Saputi,[26,49] D. Saranin,[44] A. Sarnatskiy,[78] G. Sarpis,[59] M. Sarpis,[63] C. Satriano,[36,y] A. Satta,[37] M. Saur,[6] D. Savrina,[44] H. Sazak,[17] F. Sborzacchi,[49,28] L. G. Scantlebury Smead,[64] A. Scarabotto,[19] S. Schael,[17] S. Scherl,[61] M. Schiller,[60] H. Schindler,[49] M. Schmelling,[21] B. Schmidt,[49] S. Schmitt,[17] H. Schmitz,[18] O. Schneider,[50] A. Schopper,[49] N. Schulte,[19] S. Schulte,[50] M. H. Schune,[14] R. Schwemmer,[49] G. Schwering,[17] B. Sciascia,[28] A. Sciuccati,[49] I. Segal,[76] S. Sellam,[47] A. Semennikov,[44] T. Senger,[51] M. Senghi Soares,[39] A. Sergi,[29,j] N. Serra,[51] L. Sestini,[33] A. Seuthe,[19] Y. Shang,[6] D. M. Shangase,[83] M. Shapkin,[44] R. S. Sharma,[69] I. Shchemerov,[44] L. Shchutska,[50] T. Shears,[61] L. Shekhtman,[44] Z. Shen,[6] S. Sheng,[5,7] V. Shevchenko,[44] B. Shi,[7] Q. Shi,[7] Y. Shimizu,[14] E. Shmanin,[25] R. Shorkin,[44] J. D. Shupperd,[69] R. Silva Coutinho,[69] G. Simi,[33,g] S. Simone,[24,o] N. Skidmore,[57] T. Skwarnicki,[69] M. W. Slater,[54] J. C. Smallwood,[64] E. Smith,[65] K. Smith,[68] M. Smith,[62] A. Snoch,[38] L. Soares Lavra,[59] M. D. Sokoloff,[66] F. J. P. Soler,[60] A. Solomin,[44,55] A. Solovev,[44] I. Solovyev,[44] N. S. Sommerfeld,[18] R. Song,[1] Y. Song,[50] Y. Song,[4,p] Y. S. Song,[6] F. L. Souza De Almeida,[69] B. Souza De Paula,[3] E. Spadaro Norella,[29,j] E. Spedicato,[25] J. G. Speer,[19] E. Spiridenkov,[44] P. Spradlin,[60] V. Sriskaran,[49] F. Stagni,[49] M. Stahl,[49] S. Stahl,[49] S. Stanislaus,[64] E. N. Stein,[49] O. Steinkamp,[51] O. Stenyakin,[44] H. Stevens,[19] D. Strekalina,[44] Y. Su,[7] F. Suljik,[64] J. Sun,[32] L. Sun,[74] D. Sundfeld,[2] W. Sutcliffe,[51] P. N. Swallow,[54] K. Swientek,[40] F. Swystun,[56] A. Szabelski,[42] T. Szumlak,[40] Y. Tan,[4,p] Y. Tang,[74] M. D. Tat,[64] A. Terentev,[44] F. Terzuoli,[35,49,w] F. Teubert,[49] E. Thomas,[49] D. J. D. Thompson,[54] H. Tilquin,[62] V. Tisserand,[11] S. T'Jampens,[10] M. Tobin,[5,49] L. Tomassetti,[26,f] G. Tonani,[30,49,k] X. Tong,[6] D. Torres Machado,[2] L. Toscano,[19] D. Y. Tou,[4,p] C. Trippl,[46] G. Tuci,[22] N. Tuning,[38] L. H. Uecker,[22] A. Ukleja,[40] D. J. Unverzagt,[22] B. Urbach,[59] E. Ursov,[44] A. Usachov,[39] A. Ustyuzhanin,[44] U. Uwer,[22] V. Vagnoni,[25] V. Valcarce Cadenas,[47] G. Valenti,[25] N. Valls Canudas,[49] H. Van Hecke,[68] E. van Herwijnen,[62] C. B. Van Hulse,[47,z] R. Van Laak,[50] M. van Veghel,[38] G. Vasquez,[51] R. Vazquez Gomez,[45] P. Vazquez Regueiro,[47] C. Vázquez Sierra,[47] S. Vecchi,[26] J. J. Velthuis,[55] M. Veltri,[27,aa] A. Venkateswaran,[50] M. Verdoglia,[32] M. Vesterinen,[57] D. Vico Benet,[64] P. Vidrier Villalba,[45] D. Vieira,[66] M. Vieites Diaz,[49] X. Vilasis-Cardona,[46] E. Vilella Figueras,[61] A. Villa,[25] P. Vincent,[16] F. C. Volle,[54] D. vom Bruch,[13] N. Voropaev,[44] K. Vos,[79] C. Vrahas,[59] J. Wagner,[19] J. Walsh,[35] E. J. Walton,[1,57] G. Wan,[6] C. Wang,[22] G. Wang,[8] H. Wang,[73] J. Wang,[6] J. Wang,[5] J. Wang,[4,p] J. Wang,[74] M. Wang,[30] N. W. Wang,[7] R. Wang,[55] X. Wang,[8] X. Wang,[72] X. W. Wang,[62] Y. Wang,[6] Y. W. Wang,[73] Z. Wang,[14] Z. Wang,[4,p] Z. Wang,[30] J. A. Ward,[57,1] M. Waterlaat,[49] N. K. Watson,[54] D. Websdale,[62] Y. Wei,[6] J. Wendel,[81] B. D. C. Westhenry,[55] C. White,[56] M. Whitehead,[60] E. Whiter,[54] A. R. Wiederhold,[63] D. Wiedner,[19] G. Wilkinson,[64] M. K. Wilkinson,[66] M. Williams,[65] M. J. Williams,[49] M. R. J. Williams,[59] R. Williams,[56] Z. Williams,[55] F. F. Wilson,[58] M. Winn,[12] W. Wislicki,[42] M. Witek,[41] L. Witola,[22] G. Wormser,[14] S. A. Wotton,[56] H. Wu,[69] J. Wu,[8] X. Wu,[74] Y. Wu,[6] Z. Wu,[7] K. Wyllie,[49] S. Xian,[72] Z. Xiang,[5] Y. Xie,[8] A. Xu,[35] J. Xu,[7] L. Xu,[4,p] L. Xu,[4,p] M. Xu,[57] Z. Xu,[49] Z. Xu,[7] Z. Xu,[5] K. Yang,[62] S. Yang,[7] X. Yang,[6] Y. Yang,[29,j] Z. Yang,[6] V. Yeroshenko,[14] H. Yeung,[63] H. Yin,[8] X. Yin,[7] C. Y. Yu,[6] J. Yu,[71] X. Yuan,[5] Y Yuan,[5,7] E. Zaffaroni,[50] M. Zavertyaev,[21] M. Zdybal,[41] F. Zenesini,[25,i] C. Zeng,[5,7] M. Zeng,[4,p] C. Zhang,[6] D. Zhang,[8] J. Zhang,[7] L. Zhang,[4,p] S. Zhang,[71] S. Zhang,[64] Y. Zhang,[6] Y. Z. Zhang,[4,p] Z. Zhang,[4,p] Y. Zhao,[22] A. Zharkova,[44] A. Zhelezov,[22] S. Z. Zheng,[6] X. Z. Zheng,[4,p] Y. Zheng,[7] T. Zhou,[6] X. Zhou,[8] Y. Zhou,[7] V. Zhovkovska,[57] L. Z. Zhu,[7] X. Zhu,[4,p] X. Zhu,[8] V. Zhukov,[17] J. Zhuo,[48] Q. Zou,[5,7] D. Zuliani,[33,g] and G. Zunica[50]

(LHCb Collaboration)

[1]*School of Physics and Astronomy, Monash University, Melbourne, Australia*
[2]*Centro Brasileiro de Pesquisas Físicas (CBPF), Rio de Janeiro, Brazil*
[3]*Universidade Federal do Rio de Janeiro (UFRJ), Rio de Janeiro, Brazil*

[4]Department of Engineering Physics, Tsinghua University, Beijing, China
[5]Institute of High Energy Physics (IHEP), Beijing, China
[6]School of Physics State Key Laboratory of Nuclear Physics and Technology, Peking University, Beijing, China
[7]University of Chinese Academy of Sciences, Beijing, China
[8]Institute of Particle Physics, Central China Normal University, Wuhan, Hubei, China
[9]Consejo Nacional de Rectores (CONARE), San Jose, Costa Rica
[10]Université Savoie Mont Blanc, CNRS, IN2P3-LAPP, Annecy, France
[11]Université Clermont Auvergne, CNRS/IN2P3, LPC, Clermont-Ferrand, France
[12]Université Paris-Saclay, Centre d'Etudes de Saclay (CEA), IRFU, Saclay, France, Gif-Sur-Yvette, France
[13]Aix Marseille Univ, CNRS/IN2P3, CPPM, Marseille, France
[14]Université Paris-Saclay, CNRS/IN2P3, IJCLab, Orsay, France
[15]Laboratoire Leprince-Ringuet, CNRS/IN2P3, Ecole Polytechnique, Institut Polytechnique de Paris, Palaiseau, France
[16]LPNHE, Sorbonne Université, Paris Diderot Sorbonne Paris Cité, CNRS/IN2P3, Paris, France
[17]I. Physikalisches Institut, RWTH Aachen University, Aachen, Germany
[18]Universität Bonn—Helmholtz-Institut für Strahlen und Kernphysik, Bonn, Germany
[19]Fakultät Physik, Technische Universität Dortmund, Dortmund, Germany
[20]Physikalisches Institut, Albert-Ludwigs-Universität Freiburg, Freiburg, Germany
[21]Max-Planck-Institut für Kernphysik (MPIK), Heidelberg, Germany
[22]Physikalisches Institut, Ruprecht-Karls-Universität Heidelberg, Heidelberg, Germany
[23]School of Physics, University College Dublin, Dublin, Ireland
[24]INFN Sezione di Bari, Bari, Italy
[25]INFN Sezione di Bologna, Bologna, Italy
[26]INFN Sezione di Ferrara, Ferrara, Italy
[27]INFN Sezione di Firenze, Firenze, Italy
[28]INFN Laboratori Nazionali di Frascati, Frascati, Italy
[29]INFN Sezione di Genova, Genova, Italy
[30]INFN Sezione di Milano, Milano, Italy
[31]INFN Sezione di Milano-Bicocca, Milano, Italy
[32]INFN Sezione di Cagliari, Monserrato, Italy
[33]INFN Sezione di Padova, Padova, Italy
[34]INFN Sezione di Perugia, Perugia, Italy
[35]INFN Sezione di Pisa, Pisa, Italy
[36]INFN Sezione di Roma La Sapienza, Roma, Italy
[37]INFN Sezione di Roma Tor Vergata, Roma, Italy
[38]Nikhef National Institute for Subatomic Physics, Amsterdam, Netherlands
[39]Nikhef National Institute for Subatomic Physics and VU University Amsterdam, Amsterdam, Netherlands
[40]AGH—University of Krakow, Faculty of Physics and Applied Computer Science, Kraków, Poland
[41]Henryk Niewodniczanski Institute of Nuclear Physics Polish Academy of Sciences, Kraków, Poland
[42]National Center for Nuclear Research (NCBJ), Warsaw, Poland
[43]Horia Hulubei National Institute of Physics and Nuclear Engineering, Bucharest-Magurele, Romania
[44]Authors affiliated with an institute formerly covered by a cooperation agreement with CERN
[45]ICCUB, Universitat de Barcelona, Barcelona, Spain
[46]La Salle, Universitat Ramon Llull, Barcelona, Spain
[47]Instituto Galego de Física de Altas Enerxías (IGFAE), Universidade de Santiago de Compostela, Santiago de Compostela, Spain
[48]Instituto de Fisica Corpuscular, Centro Mixto Universidad de Valencia—CSIC, Valencia, Spain
[49]European Organization for Nuclear Research (CERN), Geneva, Switzerland
[50]Institute of Physics, Ecole Polytechnique Fédérale de Lausanne (EPFL), Lausanne, Switzerland
[51]Physik-Institut, Universität Zürich, Zürich, Switzerland
[52]NSC Kharkiv Institute of Physics and Technology (NSC KIPT), Kharkiv, Ukraine
[53]Institute for Nuclear Research of the National Academy of Sciences (KINR), Kyiv, Ukraine
[54]School of Physics and Astronomy, University of Birmingham, Birmingham, United Kingdom
[55]H.H. Wills Physics Laboratory, University of Bristol, Bristol, United Kingdom
[56]Cavendish Laboratory, University of Cambridge, Cambridge, United Kingdom
[57]Department of Physics, University of Warwick, Coventry, United Kingdom
[58]STFC Rutherford Appleton Laboratory, Didcot, United Kingdom
[59]School of Physics and Astronomy, University of Edinburgh, Edinburgh, United Kingdom

[60]*School of Physics and Astronomy, University of Glasgow, Glasgow, United Kingdom*
[61]*Oliver Lodge Laboratory, University of Liverpool, Liverpool, United Kingdom*
[62]*Imperial College London, London, United Kingdom*
[63]*Department of Physics and Astronomy, University of Manchester, Manchester, United Kingdom*
[64]*Department of Physics, University of Oxford, Oxford, United Kingdom*
[65]*Massachusetts Institute of Technology, Cambridge, Massachusetts, USA*
[66]*University of Cincinnati, Cincinnati, Ohio, USA*
[67]*University of Maryland, College Park, Maryland, USA*
[68]*Los Alamos National Laboratory (LANL), Los Alamos, New Mexico, USA*
[69]*Syracuse University, Syracuse, New York, USA*
[70]*Pontifícia Universidade Católica do Rio de Janeiro (PUC-Rio), Rio de Janeiro, Brazil (associated with Universidade Federal do Rio de Janeiro (UFRJ), Rio de Janeiro, Brazil)*
[71]*School of Physics and Electronics, Hunan University, Changsha City, China (associated with Institute of Particle Physics, Central China Normal University, Wuhan, Hubei, China)*
[72]*Guangdong Provincial Key Laboratory of Nuclear Science, Guangdong-Hong Kong Joint Laboratory of Quantum Matter, Institute of Quantum Matter, South China Normal University, Guangzhou, China (associated with Department of Engineering Physics, Tsinghua University, Beijing, China)*
[73]*Lanzhou University, Lanzhou, China (associated with Institute Of High Energy Physics (IHEP), Beijing, China)*
[74]*School of Physics and Technology, Wuhan University, Wuhan, China (associated with Department of Engineering Physics, Tsinghua University, Beijing, China)*
[75]*Departamento de Fisica, Universidad Nacional de Colombia, Bogota, Colombia (associated with LPNHE, Sorbonne Université, Paris Diderot Sorbonne Paris Cité, CNRS/IN2P3, Paris, France)*
[76]*Ruhr Universitaet Bochum, Fakultaet f. Physik und Astronomie, Bochum, Germany (associated with Fakultät Physik, Technische Universität Dortmund, Dortmund, Germany)*
[77]*Eotvos Lorand University, Budapest, Hungary (associated with European Organization for Nuclear Research (CERN), Geneva, Switzerland)*
[78]*Van Swinderen Institute, University of Groningen, Groningen, Netherlands (associated with Nikhef National Institute for Subatomic Physics, Amsterdam, Netherlands)*
[79]*Universiteit Maastricht, Maastricht, Netherlands (associated with Nikhef National Institute for Subatomic Physics, Amsterdam, Netherlands)*
[80]*Tadeusz Kosciuszko Cracow University of Technology, Cracow, Poland (associated with Henryk Niewodniczanski Institute of Nuclear Physics Polish Academy of Sciences, Kraków, Poland)*
[81]*Universidade da Coruña, A Coruña, Spain (associated with La Salle, Universitat Ramon Llull, Barcelona, Spain)*
[82]*Department of Physics and Astronomy, Uppsala University, Uppsala, Sweden (associated with Institution School of Physics and Astronomy, University of Glasgow, Glasgow, United Kingdom)*
[83]*University of Michigan, Ann Arbor, Michigan, USA (associated with Syracuse University, Syracuse, New York, USA)*

[a]Deceased.
[b]Also at Lamarr Institute for Machine Learning and Artificial Intelligence, Dortmund, Germany.
[c]Also at Università degli Studi di Milano-Bicocca, Milano, Italy.
[d]Also at Università di Roma Tor Vergata, Roma, Italy.
[e]Also at Scuola Normale Superiore, Pisa, Italy.
[f]Also at Università di Ferrara, Ferrara, Italy.
[g]Also at Università di Padova, Padova, Italy.
[h]Also at Facultad de Ciencias Fisicas, Madrid, Spain.
[i]Also at Università di Bologna, Bologna, Italy.
[j]Also at Università di Genova, Genova, Italy.
[k]Also at Università degli Studi di Milano, Milano, Italy.
[l]Also at Universidad Nacional Autónoma de Honduras, Tegucigalpa, Honduras.
[m]Also at Università di Cagliari, Cagliari, Italy.
[n]Also at Centro Federal de Educacão Tecnológica Celso Suckow da Fonseca, Rio De Janeiro, Brazil.
[o]Also at Università di Bari, Bari, Italy.
[p]Also at Center for High Energy Physics, Tsinghua University, Beijing, China.
[q]Also at Università di Perugia, Perugia, Italy.

[r]Also at LIP6, Sorbonne Université, Paris, France.
[s]Also at Università di Pisa, Pisa, Italy.
[t]Also at Hangzhou Institute for Advanced Study, UCAS, Hangzhou, China.
[u]Also at School of Physics and Electronics, Henan University, Kaifeng, China.
[v]Also at Università di Bergamo, Bergamo, Italy.
[w]Also at Università di Siena, Siena, Italy.
[x]Also at Department of Physics/Division of Particle Physics, Lund, Sweden.
[y]Also at Università della Basilicata, Potenza, Italy.
[z]Also at Universidad de Alcalá, Alcalá de Henares, Spain.
[aa]Also at Università di Urbino, Urbino, Italy.